

Low-temperature-meltable elastomers based on linear polydimethylsiloxane chains alpha,omega-terminated with mesogenic groups as physical crosslinker: A passive smart material with potential as viscoelastic coupling. Part II: Viscoelastic and rheological properties

Sabina Horodecka^{1,2}, Adam Strachota^{1*}, Beata Mossety-Leszczak³, Maciej Kisiel³, Beata Strachota¹, Miroslav Šlouf¹

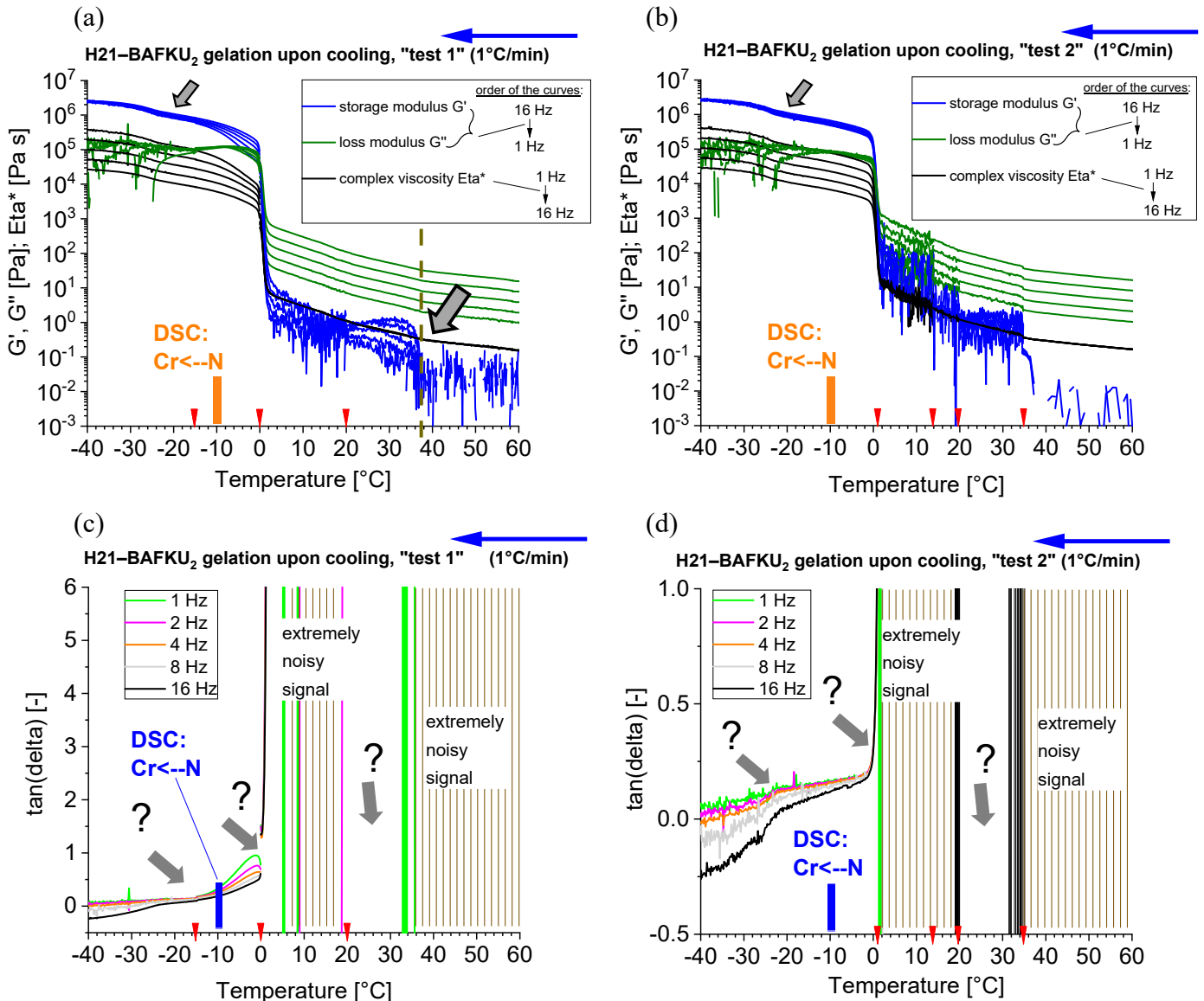
¹⁾ Institute of Macromolecular Chemistry, Czech Academy of Sciences,
Heyrovského nam. 2, CZ-162 06 Praha, Czech Republic

²⁾ Faculty of Science, Charles University,
Albertov 6, CZ-128 00 Praha 2, Czech Republic

³⁾ Faculty of Chemistry, Rzeszow University of Technology,
al. Powstancow Warszawy 6, PL-35-959 Rzeszow, Poland

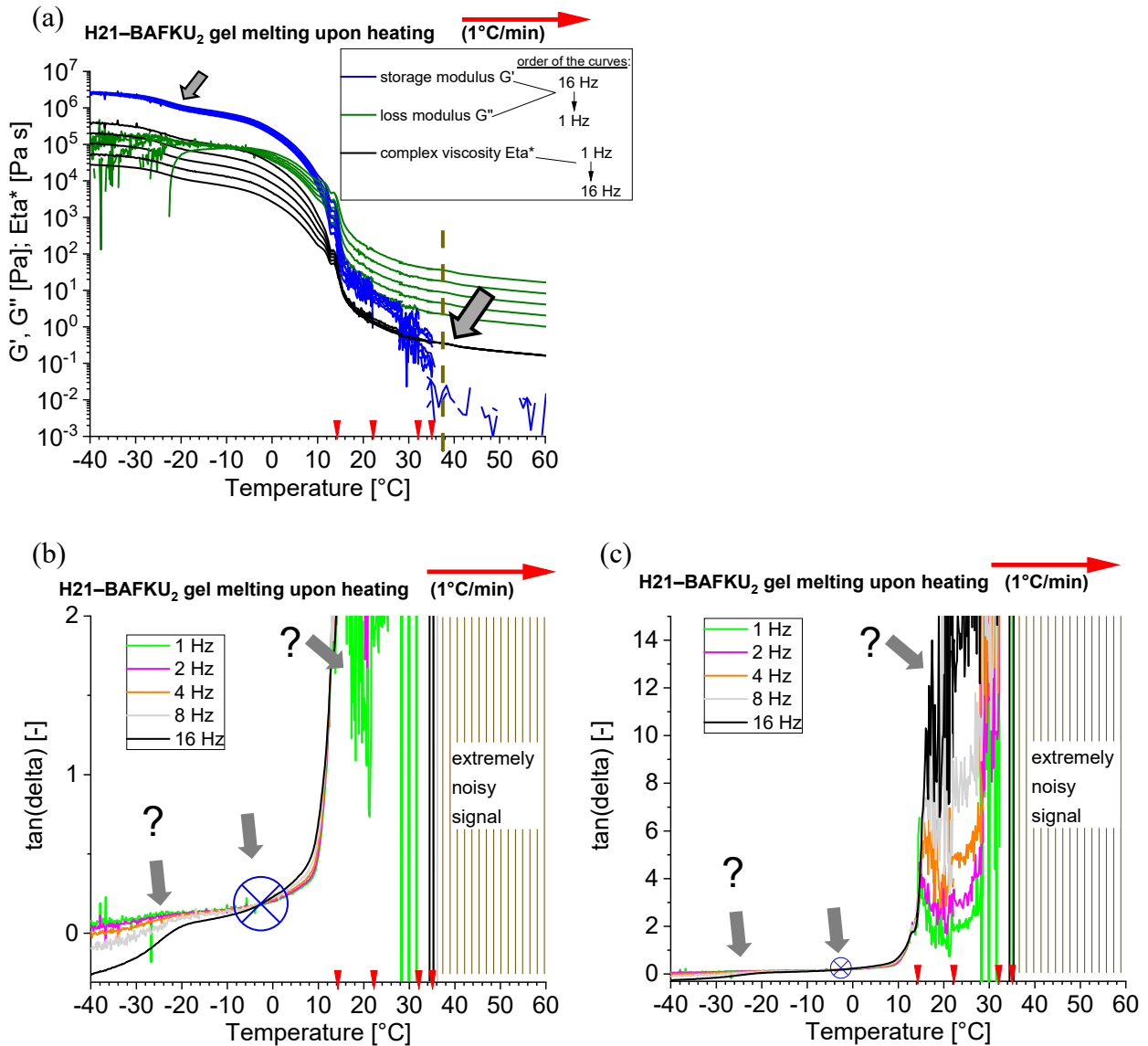
1. Gelation study via T-dependent multi-frequency rheology experiments

H21-BAFKU₂ cooling scan



SI-Fig. 1: Multi-frequency temperature ramp tests - **cooling scans** - carried out in the rubbery and melt temperature regions of H21-BAFKU₂: (a), (b): temperature dependence of the storage shear moduli G' , of the loss moduli G'' , of the complex viscosities η^* recorded at the simultaneously applied frequencies of 1, 2, 4, 8 and 16 Hz; (c), (d): sets of the $\tan \delta$ curves with marked crossover (or near-crossover) points; (a), (c): cooling scan conducted with **high deformation amplitudes**; (b), (d): cooling scan conducted with **low deformation amplitudes**; red dotted lines indicate change in strain.

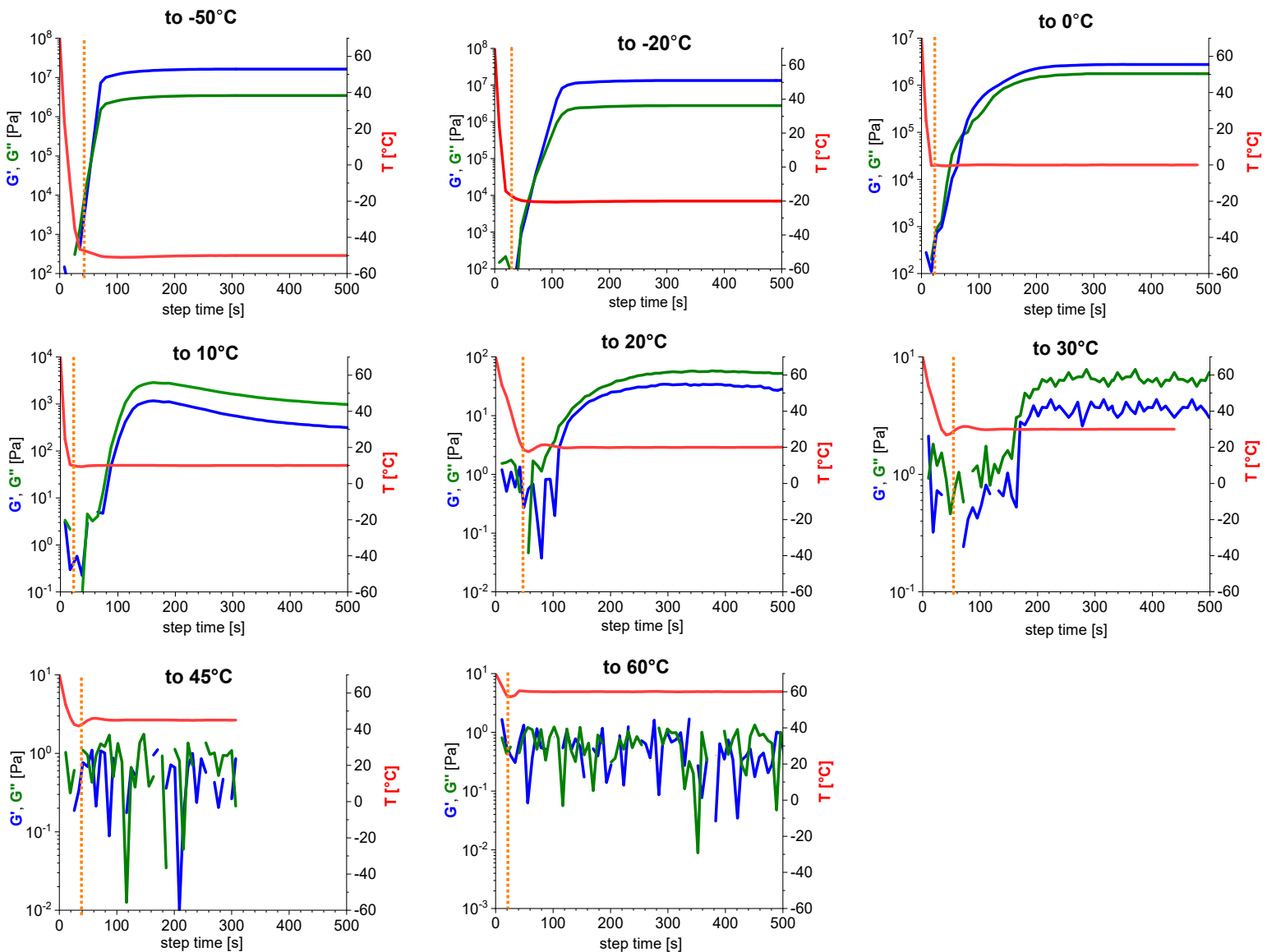
H21-BAFKU₂ heating scan



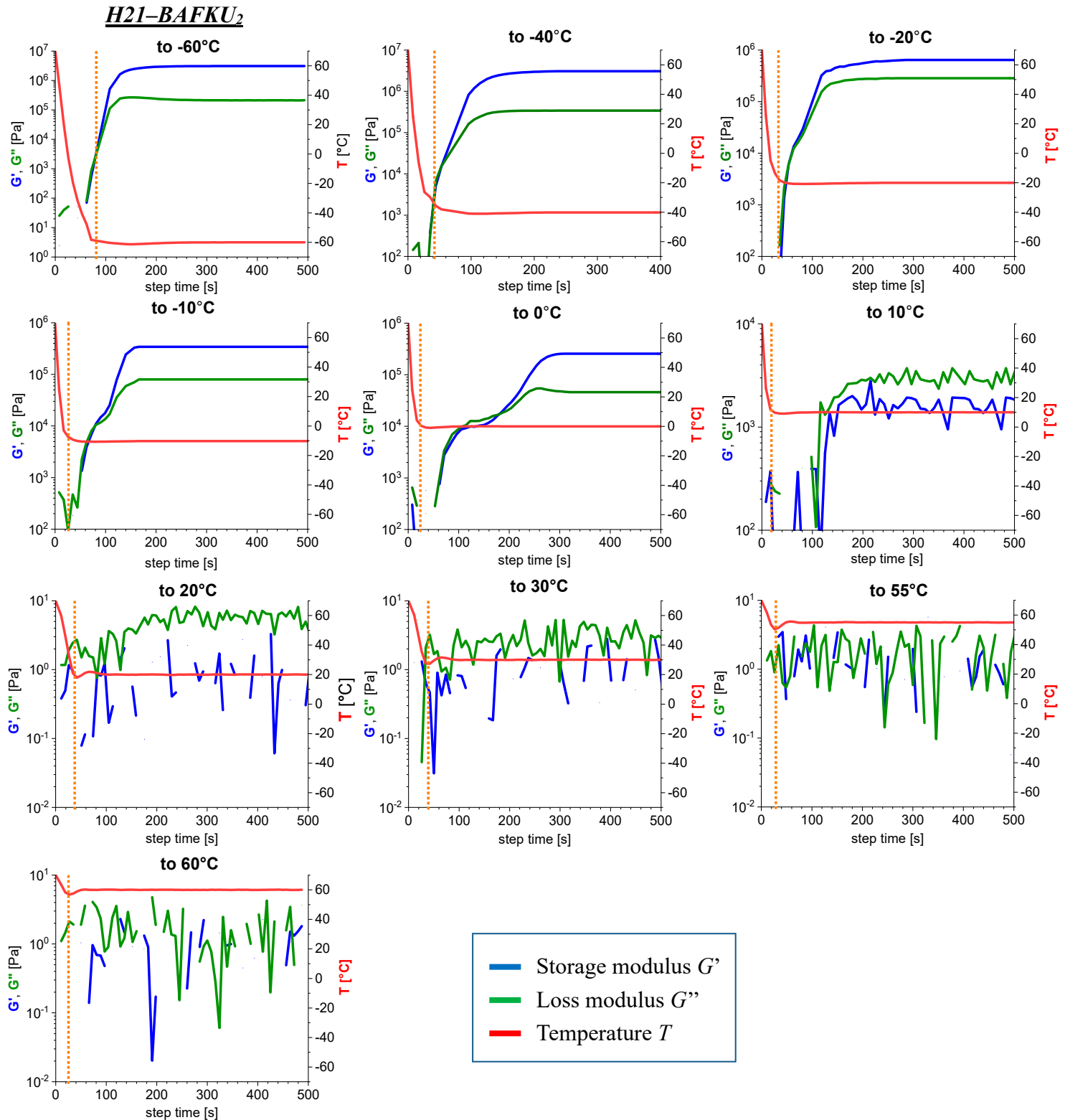
SI-Fig. 2: Multi-frequency temperature ramp test - heating scan - carried out in the rubbery and melt temperature regions of H21-BAFKU₂: (a): temperature dependence of the storage shear moduli G' , of the loss moduli G'' , of the complex viscosities η^* recorded at the simultaneously applied frequencies of 1, 2, 4, 8 and 16 Hz as heating scan; (b): sets of the $\tan \delta$ curves with marked crossover (or near-crossover) points as heating scan; (c): a different zoom of the image (b); red dotted lines indicate change in strain.

2. Kinetics of gelation upon abrupt cooling of melt

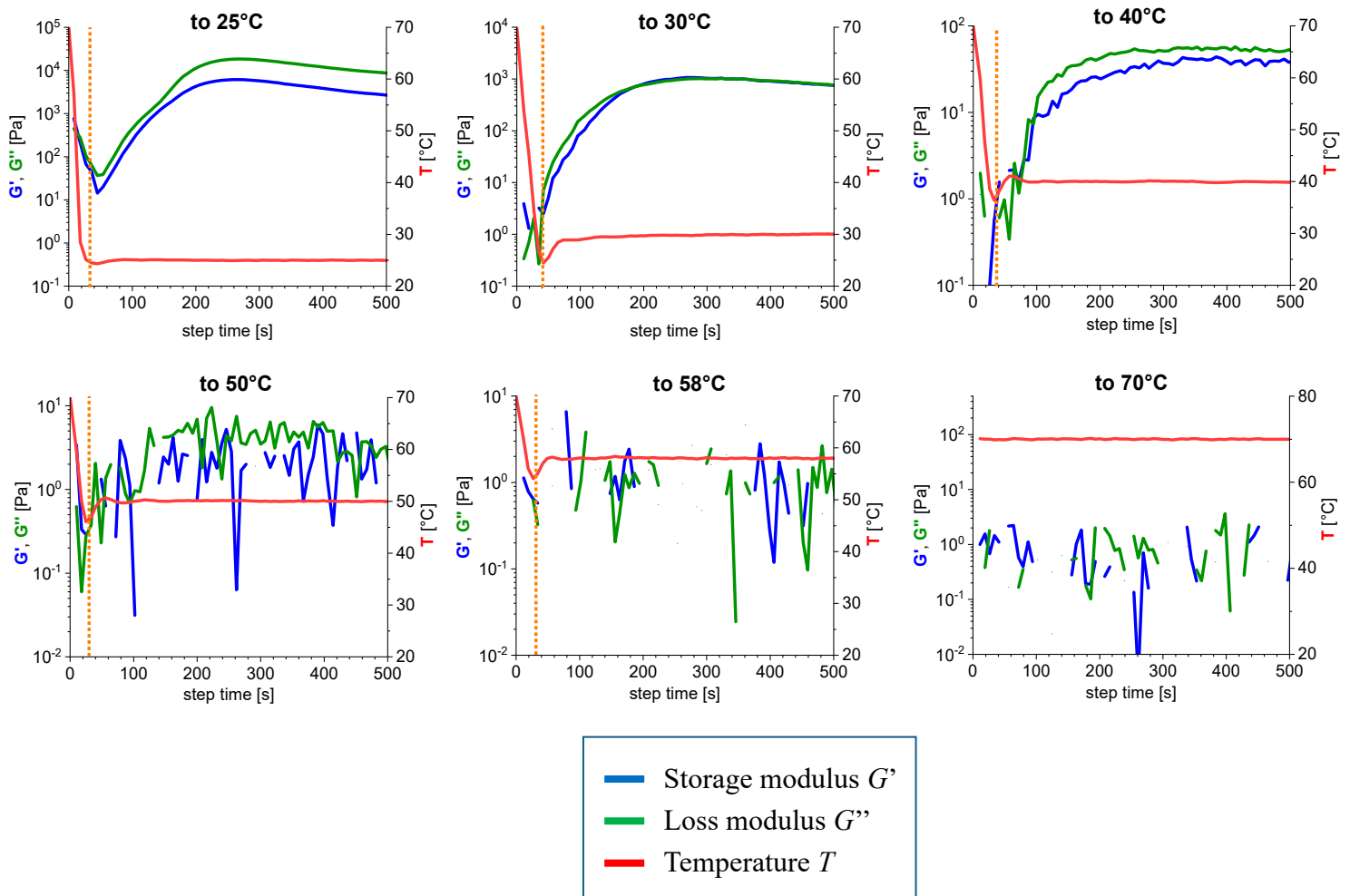
H11-BAFKU₂ : all graphs



SI-Fig. 3: Full data set: **Kinetics of the change in storage (G') and loss (G'') modulus (kinetics of physical gelation) upon cooling molten H11-BAFKU₂ from 70°C down to different temperatures ranging between -50°C and $+60^\circ\text{C}$; the course of the temperature of the plates between which the sample was loaded is also depicted.**



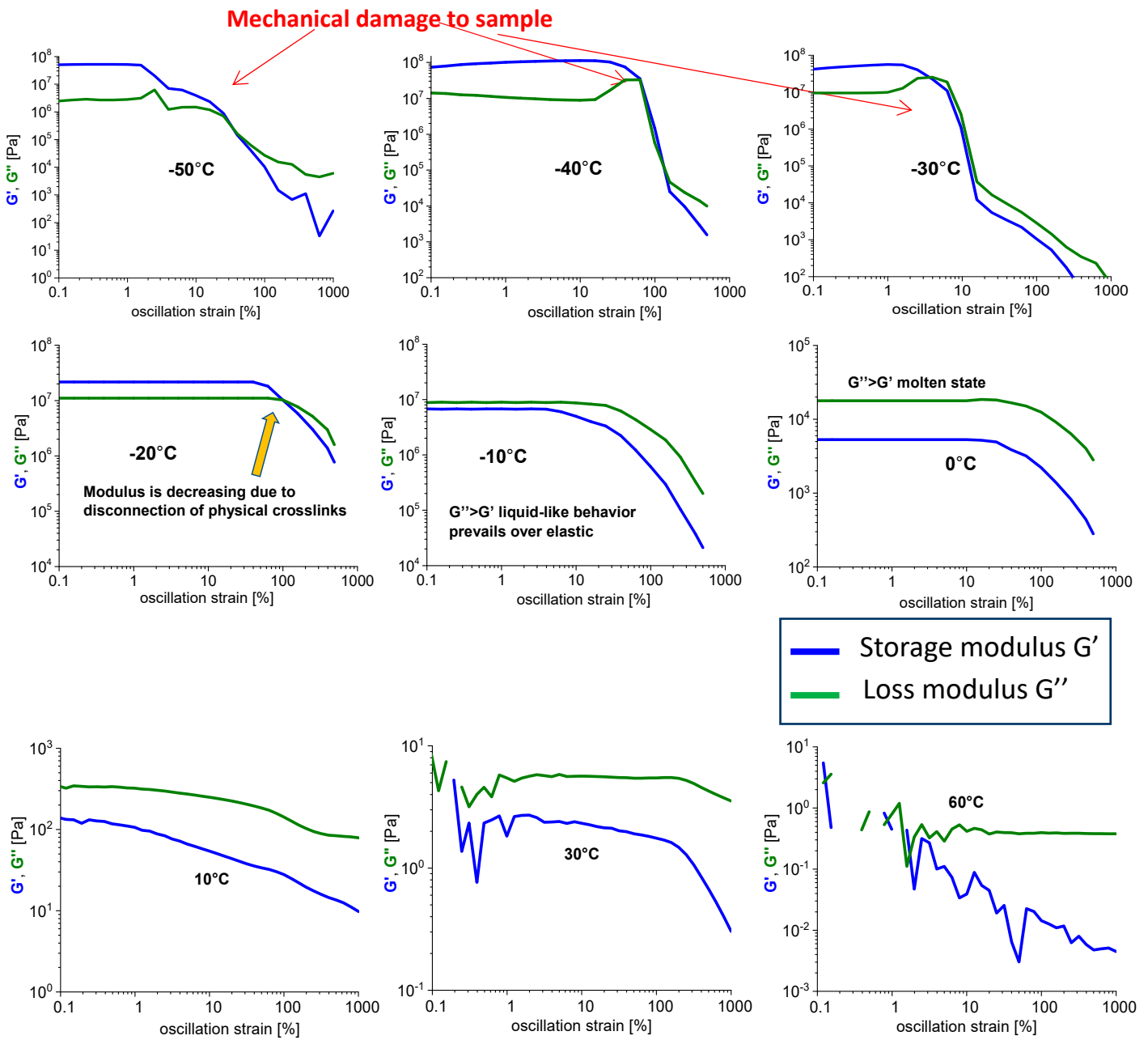
SI-Fig. 4: Kinetics of the change in storage (G') and loss (G'') modulus (kinetics of physical gelation) upon cooling molten H21-BAFKU₂ from 70°C to different temperatures ranging between -60°C and 60°C; the course of the temperature of the plates between which the sample was loaded is also depicted.

H03–BAFKU₂

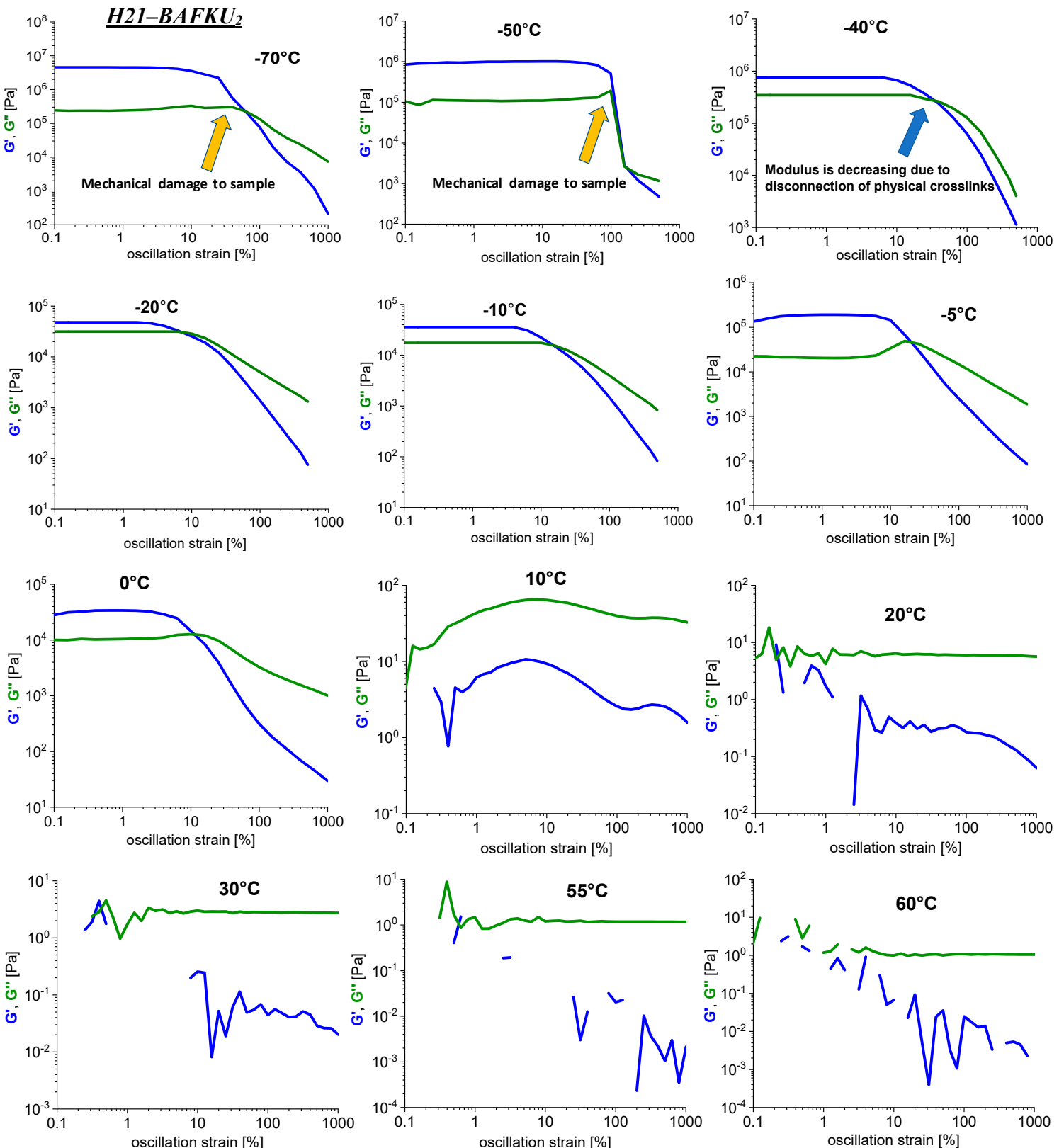
SI-Fig. 5: Kinetics of the change in storage (G') and loss (G'') modulus (kinetics of physical gelation) upon cooling molten **H03–BAFKU₂** from 70°C down to different temperatures ranging between +30°C and +70°C; the course of the temperature of the plates between which the sample was loaded is also depicted.

3. Disconnection of the physical network by high mechanical strain

H11-BAFKU₂

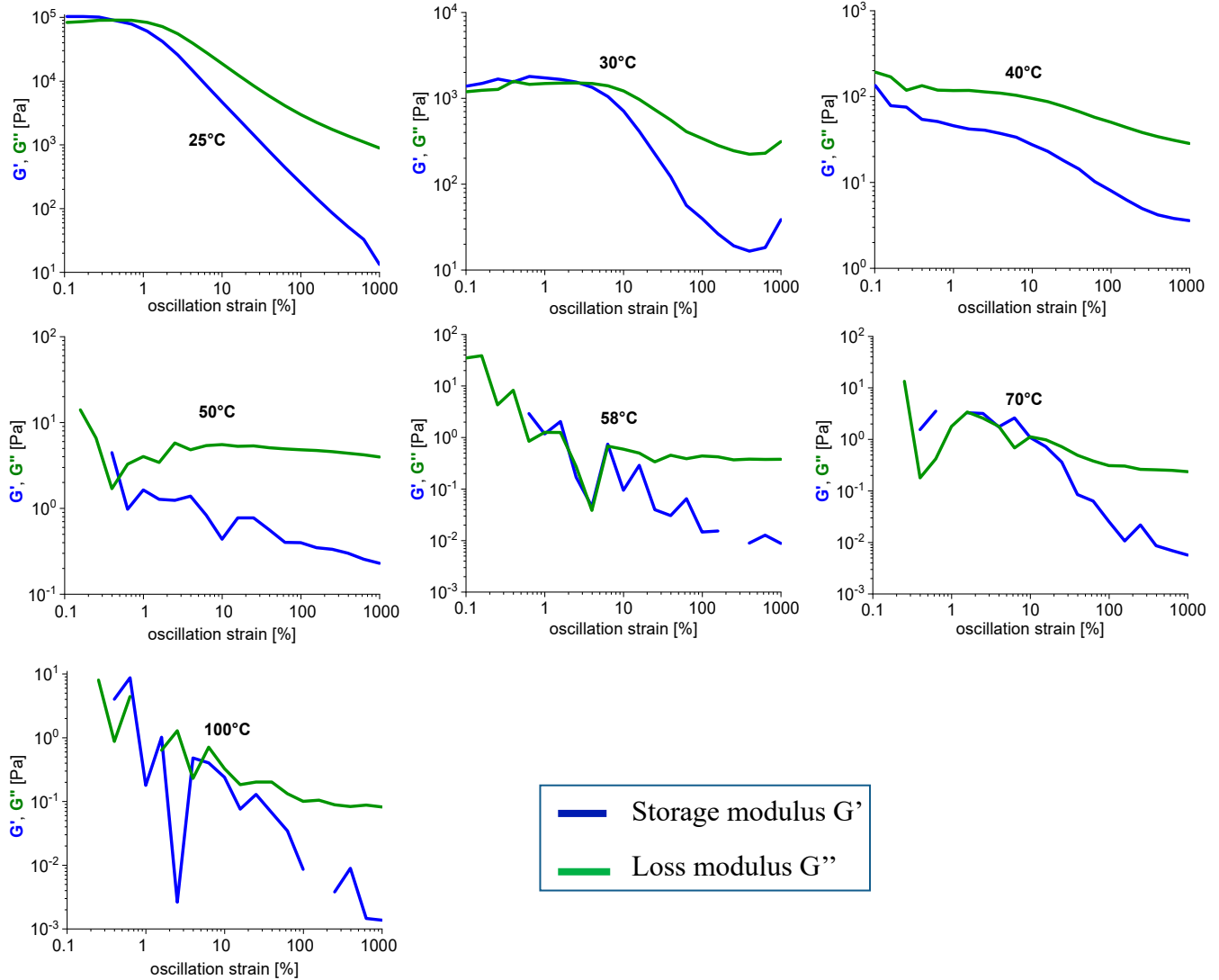


SI-Fig. 6: All data: Disconnection of the physical crosslinks in H11-BAFKU₂ by mechanical strain: strain-dependence of storage (G') and loss (G'') modulus of H21-BAFKU₂ at the temperatures from -50 to +60°C.



SI-Fig. 7: Disconnection of the physical crosslinks in H21-BAFKU₂ by mechanical strain: strain-dependence of storage (G') and loss (G'') modulus of H21-BAFKU₂ at the temperatures from -70 to +60°C.

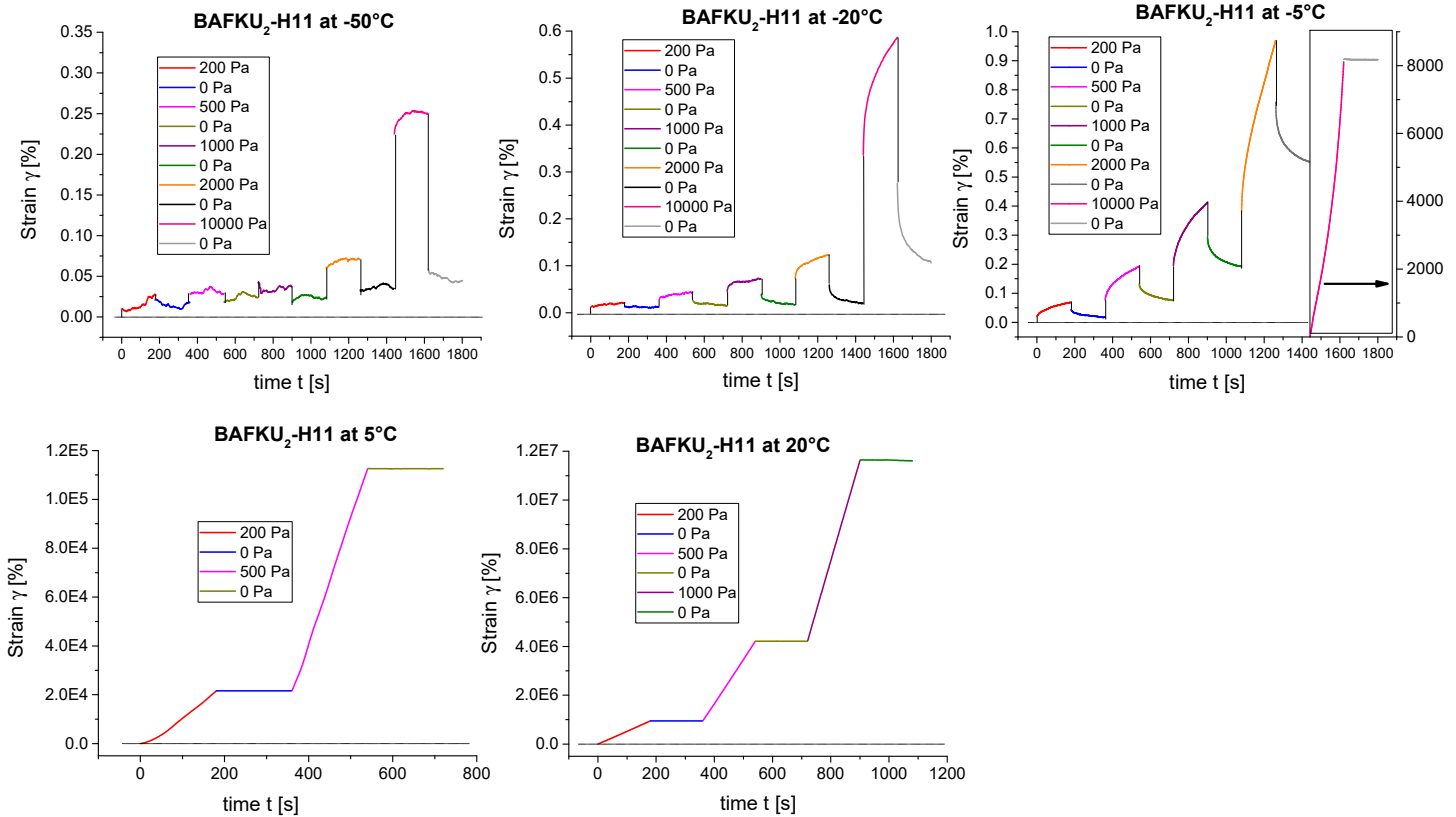
—	Storage modulus G'
—	Loss modulus G''

H03–BAFKU₂

SI-Fig. 8: Disconnection of residual physical crosslinks in H03–BAFKU₂ melt by mechanical strain: strain-dependence of storage (G') and loss (G'') modulus of H03–BAFKU₂ at the temperatures from +25 to +100°C.

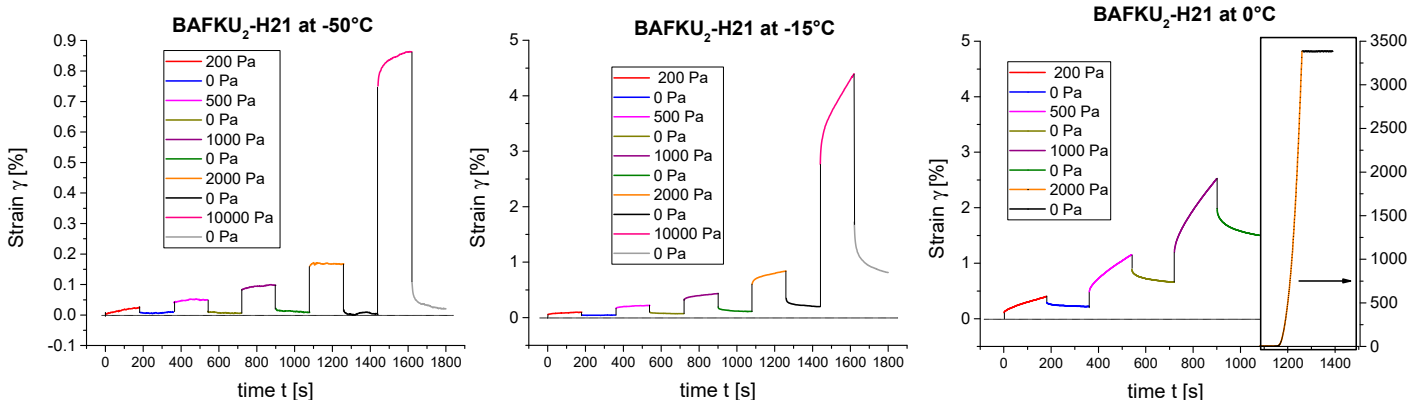
Creep tests

H11-BAFKU2 all data



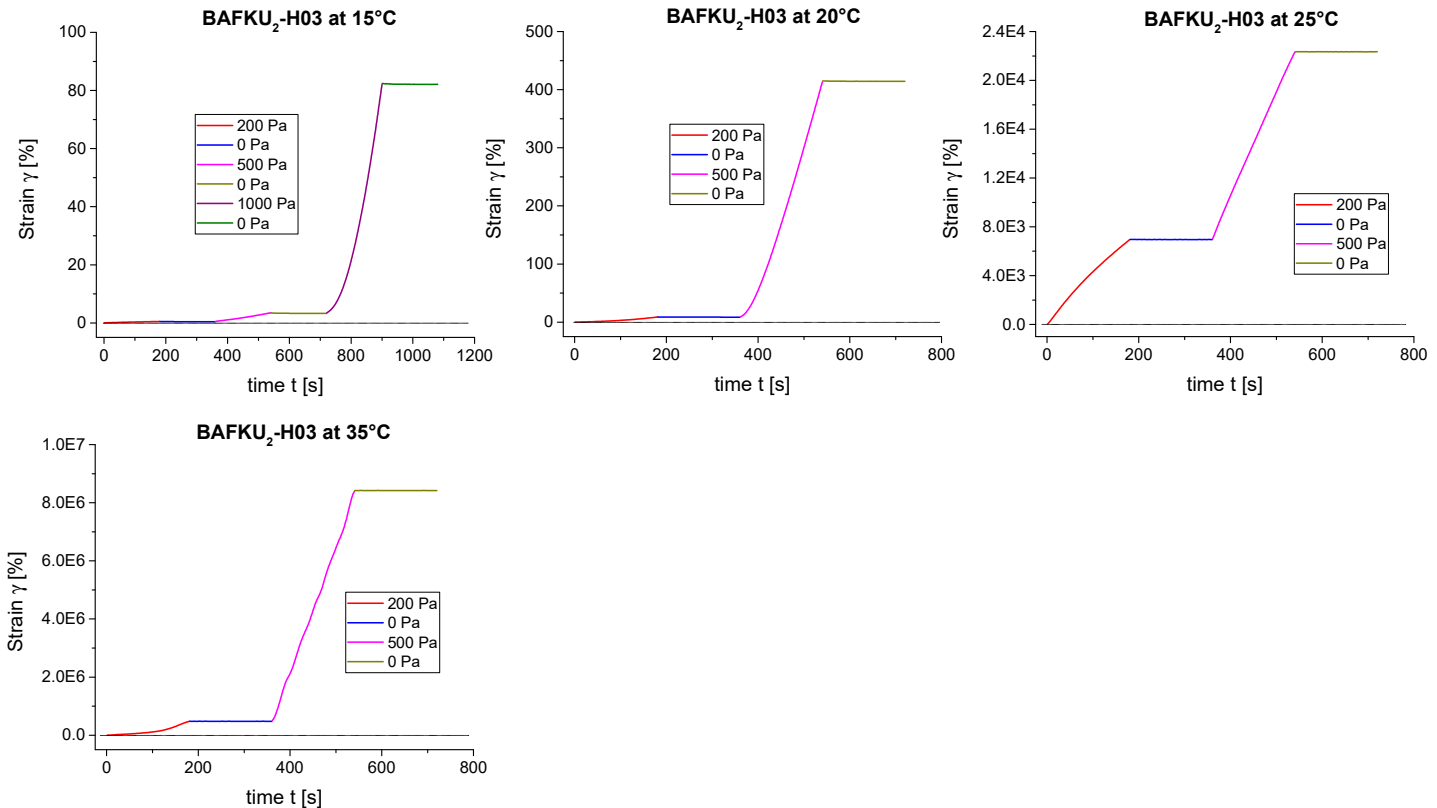
SI-Fig. 9: Multi-step creep tests of H11–BAFKU₂ all data: tests at temperatures between -50 and +20°C; stresses ranging between 200 and 10 000 Pa were applied, followed by recovery steps (at 0 Pa).

H21-BAFKU2



SI-Fig. 10: Multi-step creep tests of H21-BAFKU₂ at temperatures between -50 and 0°C; stresses ranging between 200 and 10 000 Pa were applied, followed by recovery steps (at 0 Pa).

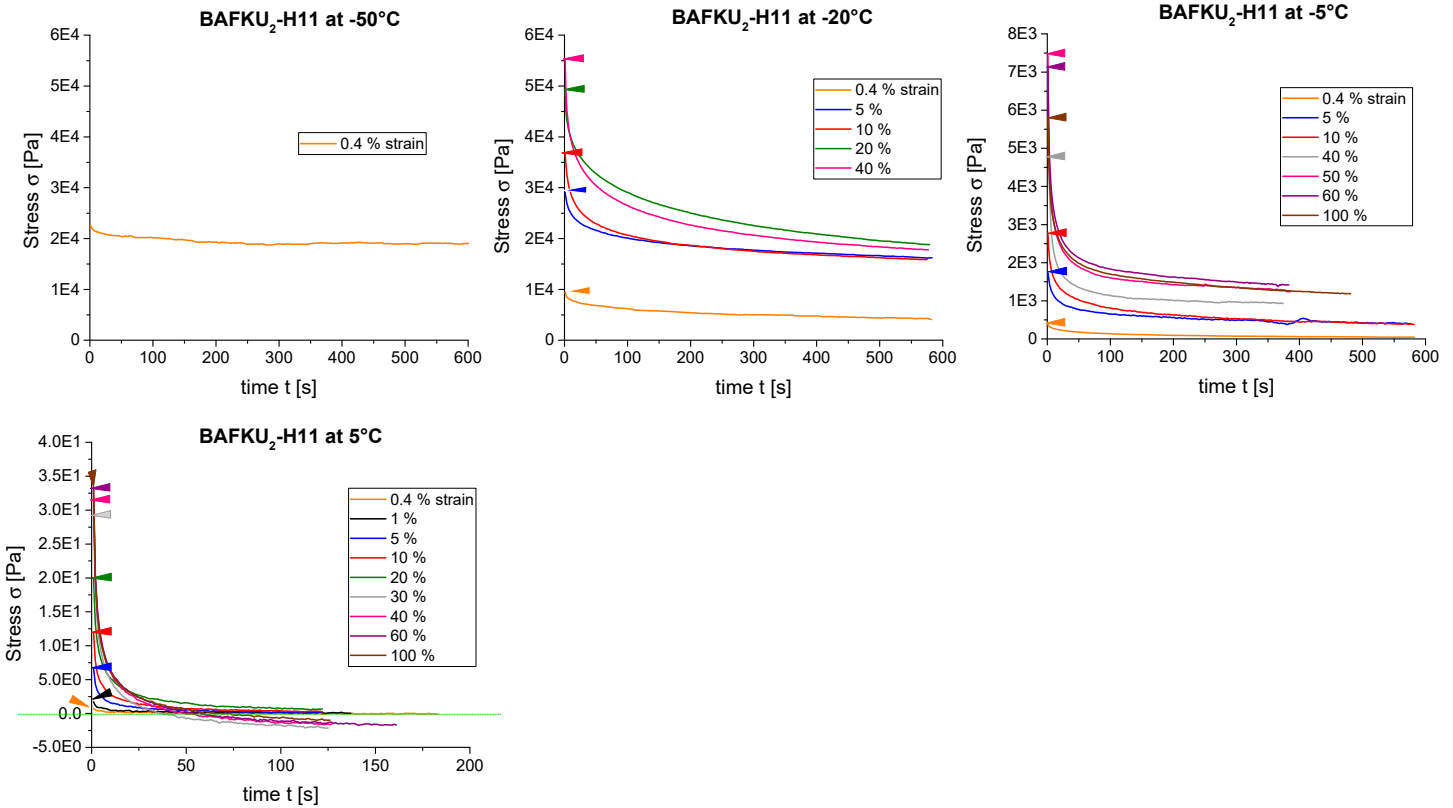
H03-BAFKU2



SI-Fig. 11: Multi-step creep tests of H03-BAFKU2 at temperatures between +15 and +35°C; stresses ranging between 200 and 1 000 Pa were applied, followed by recovery steps (at 0 Pa).

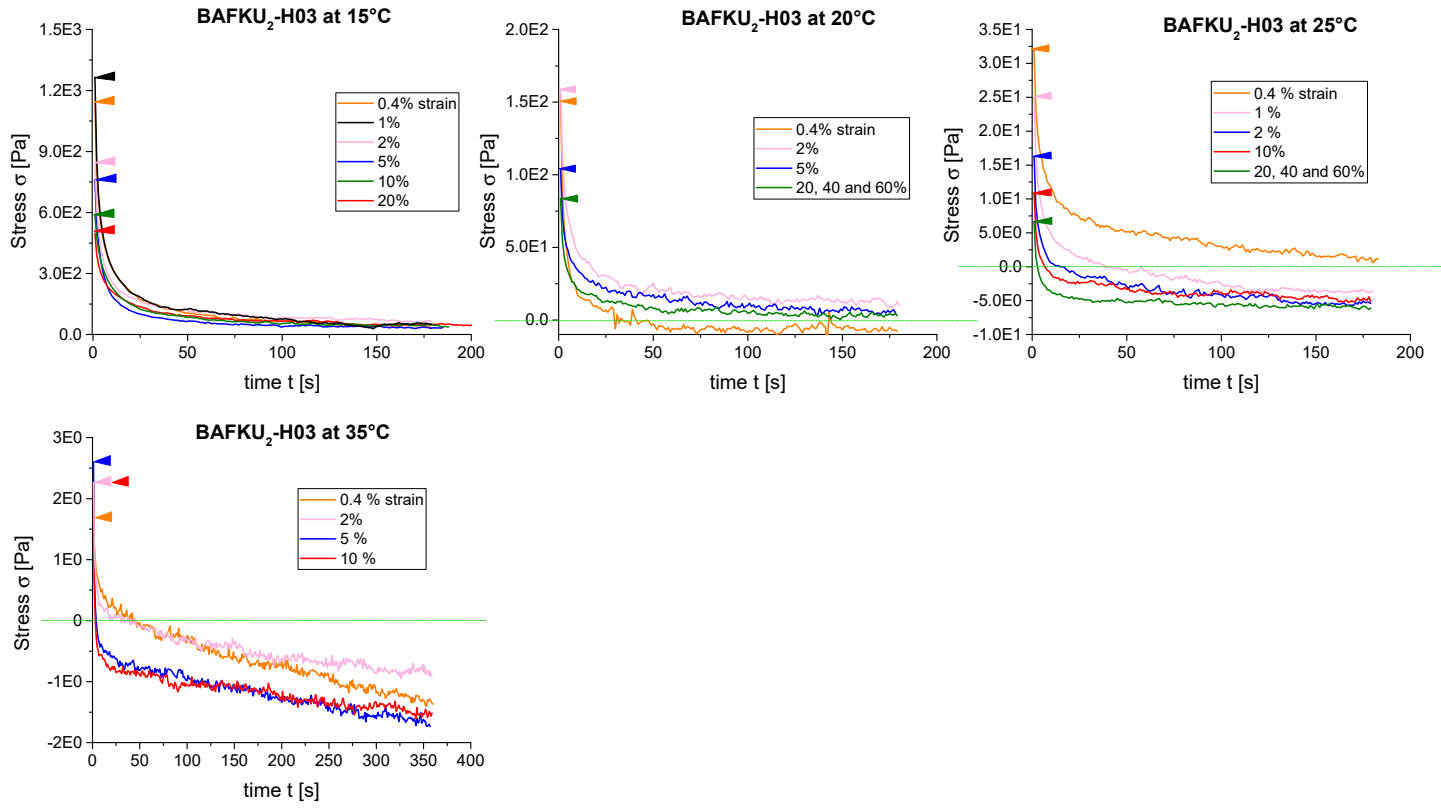
Relaxation tests

H11-BAFKU2



SI-Fig. 12: Stress relaxation tests of H11–BAFKU₂ at temperatures between -50 and +5°C; at each temperature, several constant strain values were applied.

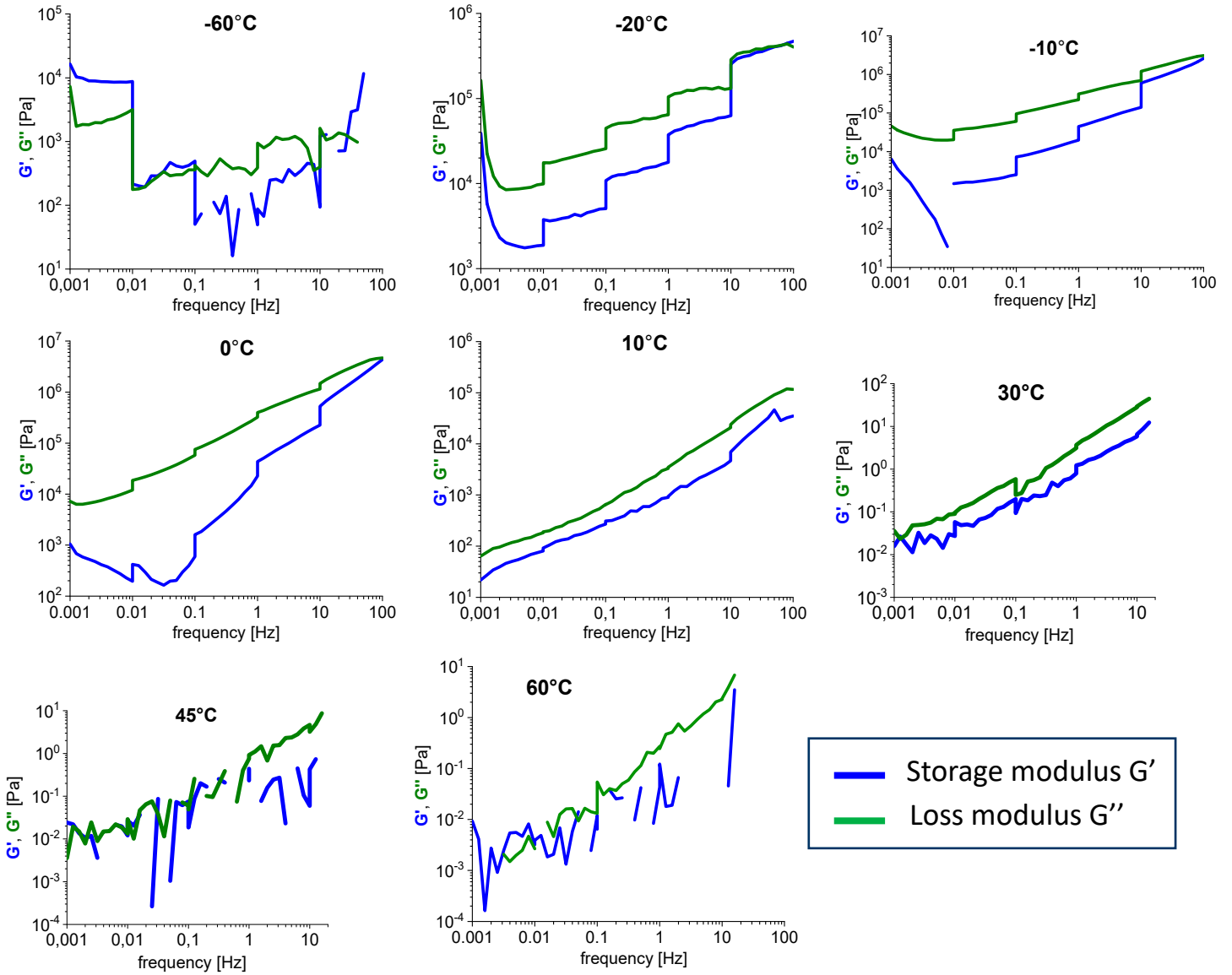
Relaxation H03-BAFKU2



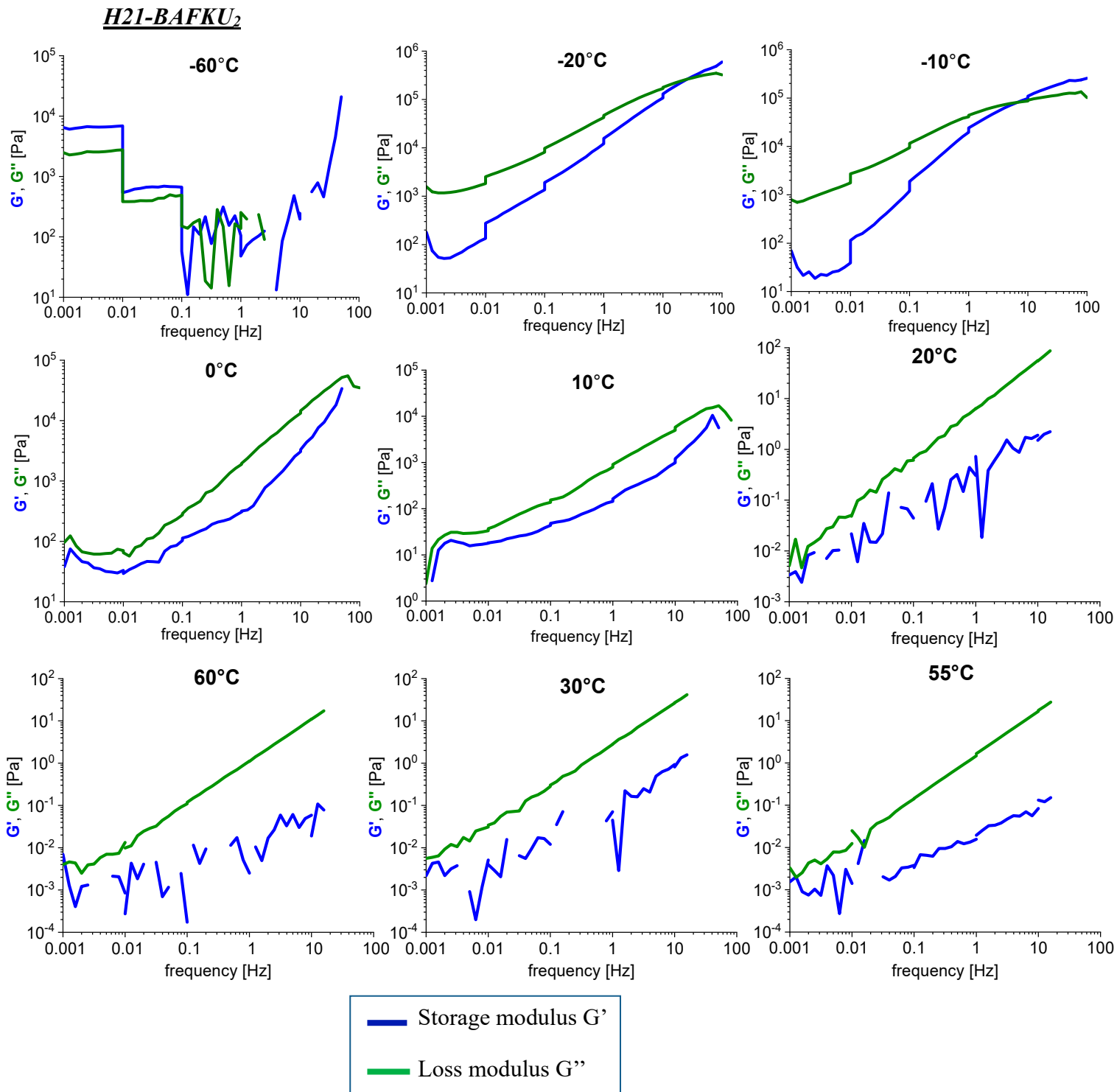
SI-Fig. 13: Stress relaxation tests of H03–BAFKU₂ at temperatures between +15 and +35°C; at each temperature, several constant strain values were applied.

4. High-frequency stiffening and self-healing effects

H11–BAFKU₂

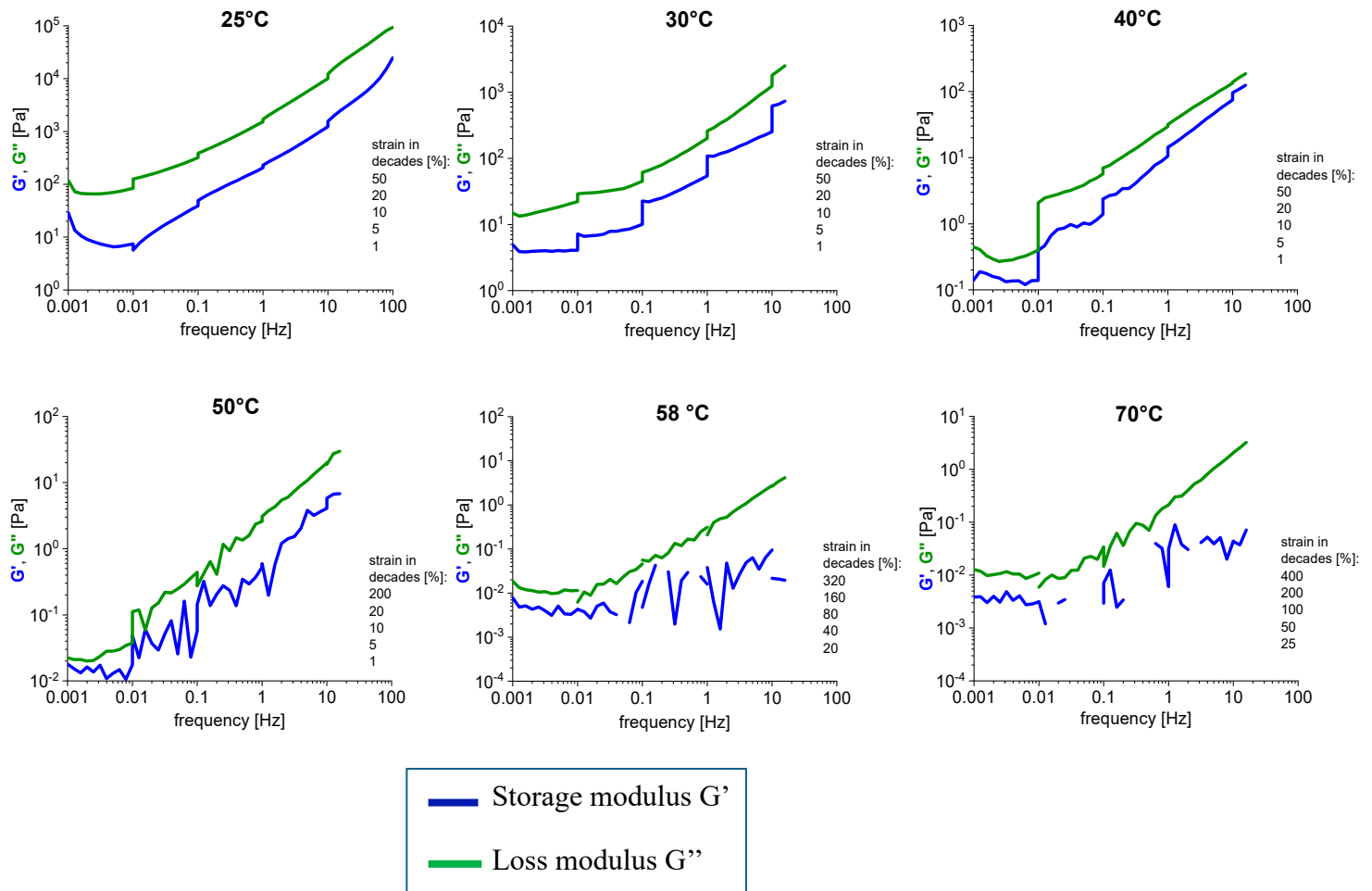


SI-Fig. 14: All data: Frequency-stiffening of H11–BAFKU₂ observed in frequency sweep tests (1 mHz to 100 Hz) conducted at temperatures between -60 and +60°C; the strain amplitude was different in each frequency decade, ranging from 50% at 1 mHz to 1% at 100 Hz; the effect of strain-induced damage to the network, as well as of its recovery between the frequency decades is clearly visible, especially in case of G' curves at lower temperatures.



SI-Fig. 15: Frequency-stiffening of H21-BAFKU₂ observed in frequency sweep tests (1 mHz to 100 Hz) conducted between -60 and +55°C; the strain amplitude was different in each frequency decade, ranging from 50% at 1 mHz to 1% at 100 Hz; the effect of strain-induced damage to the network, as well as of its recovery between the frequency decades is clearly visible, especially in case of G' curves at lower temperatures.

H03-BAFKU₂



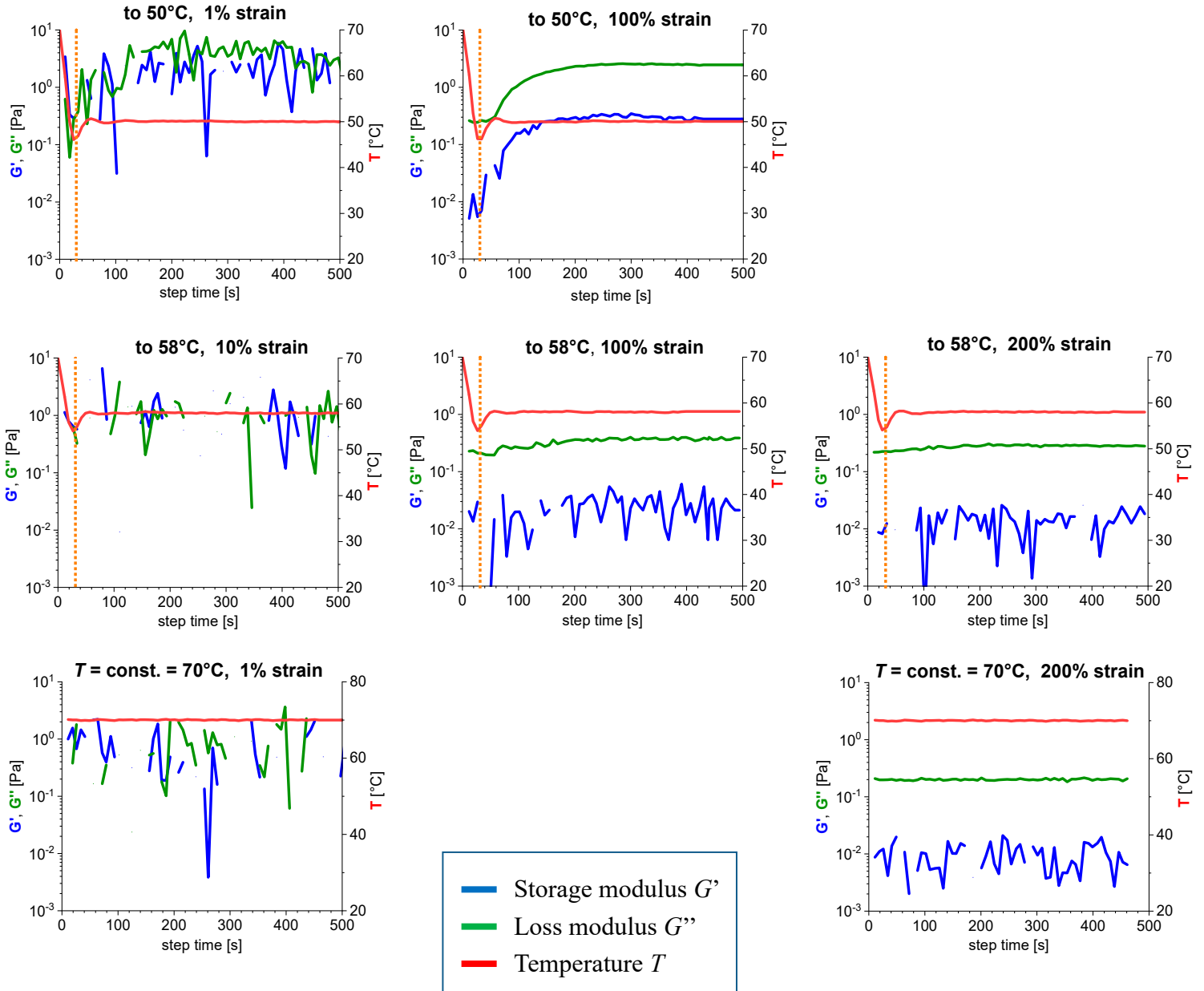
SI-Fig. 16: Frequency-stiffening of H03-BAFKU₂ melt observed in frequency sweep tests (1 mHz to 100 Hz) conducted at temperatures between +25 and +70°C; the strain amplitude was different in each frequency decade, ranging from 50% at 1 mHz to 1% at 100 Hz; the effect of strain-induced damage to elastic structures in the melt, as well as their recovery between the frequency decades is clearly visible, especially at lower temperatures.

Explanation of the upward steps in G''

While simple self-healing should lead to decrease in G'' (stronger elastomer character due to more crosslinks, shorter elastic chains and hence less friction), the experimentally observed upward steps in G'' could be explained by resistance caused by re-assembled larger aggregates (lamellae) of BAFKU, which have time to disconnect at lower frequencies (and high applied strains). Their gradual destruction by shear generates resistance (high G'' value), but also leads to a decrease in the number of these secondary aggregates and thus in turn to less than maximum resistance (smaller growth, or in extreme cases even local decrease in G''). During the experimental delay, the smaller BAFKU aggregates ('fragments') re-assemble to larger ones again, and hence can generate considerably increased resistance after the delay (upward step in G'').

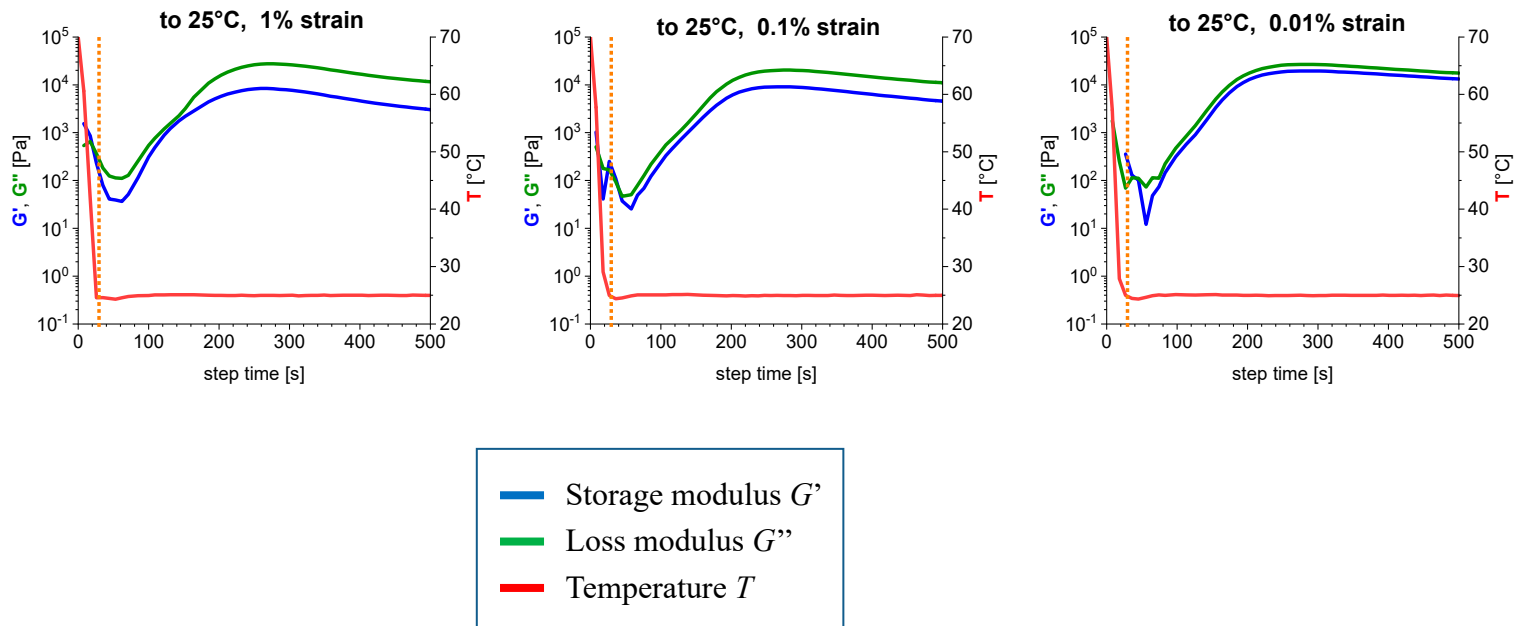
5. Thixotropy effects

H03-BAFKU₂ kinetics of gelation upon cooling



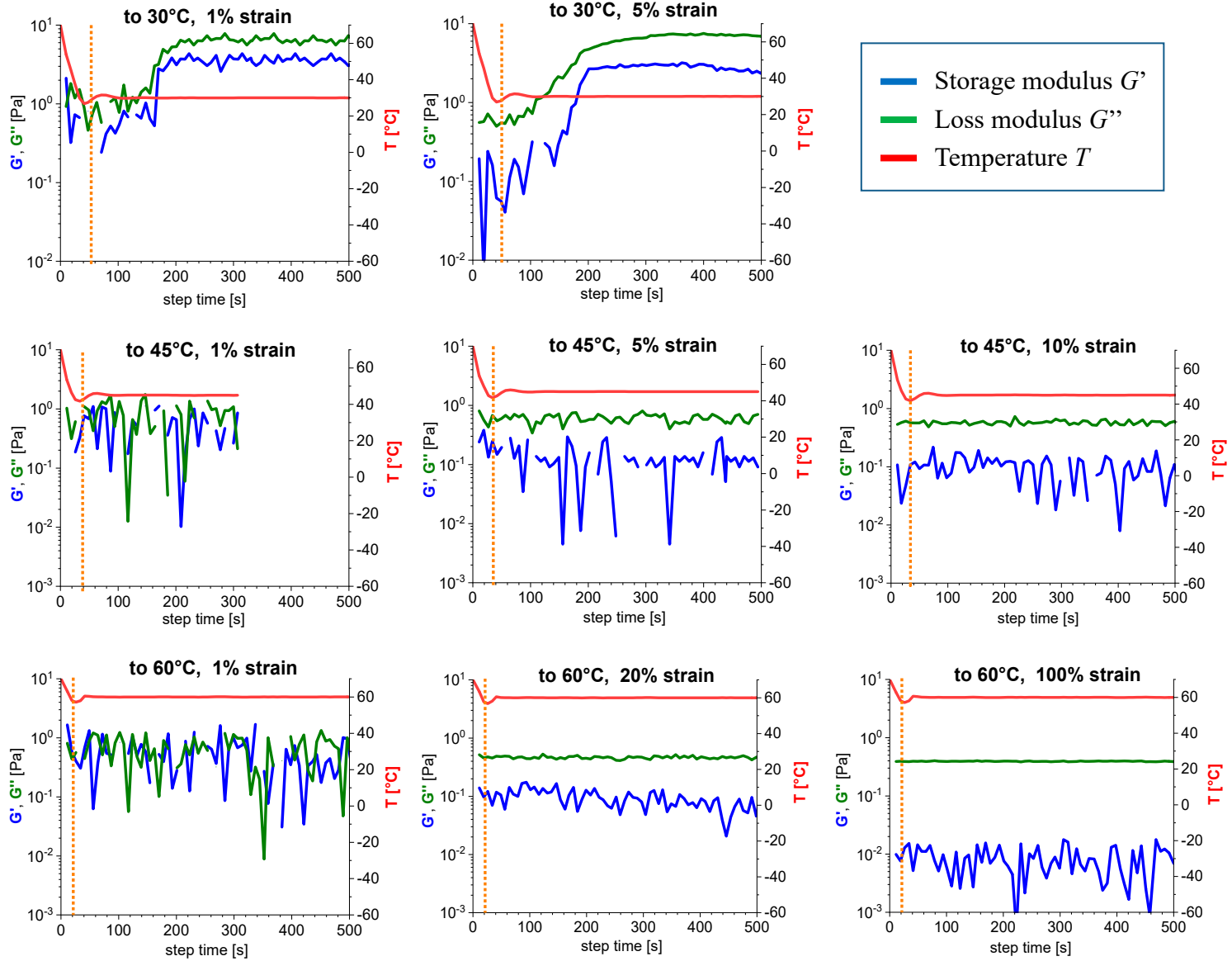
SI-Fig. 17: Thixotropy effects visible as strong strain-dependence of the moduli values (G' , G'') in case of the kinetics of physical gelation of molten H03-BAFKU₂ upon abrupt cooling.

Very small strains also lead to change in measured moduli:



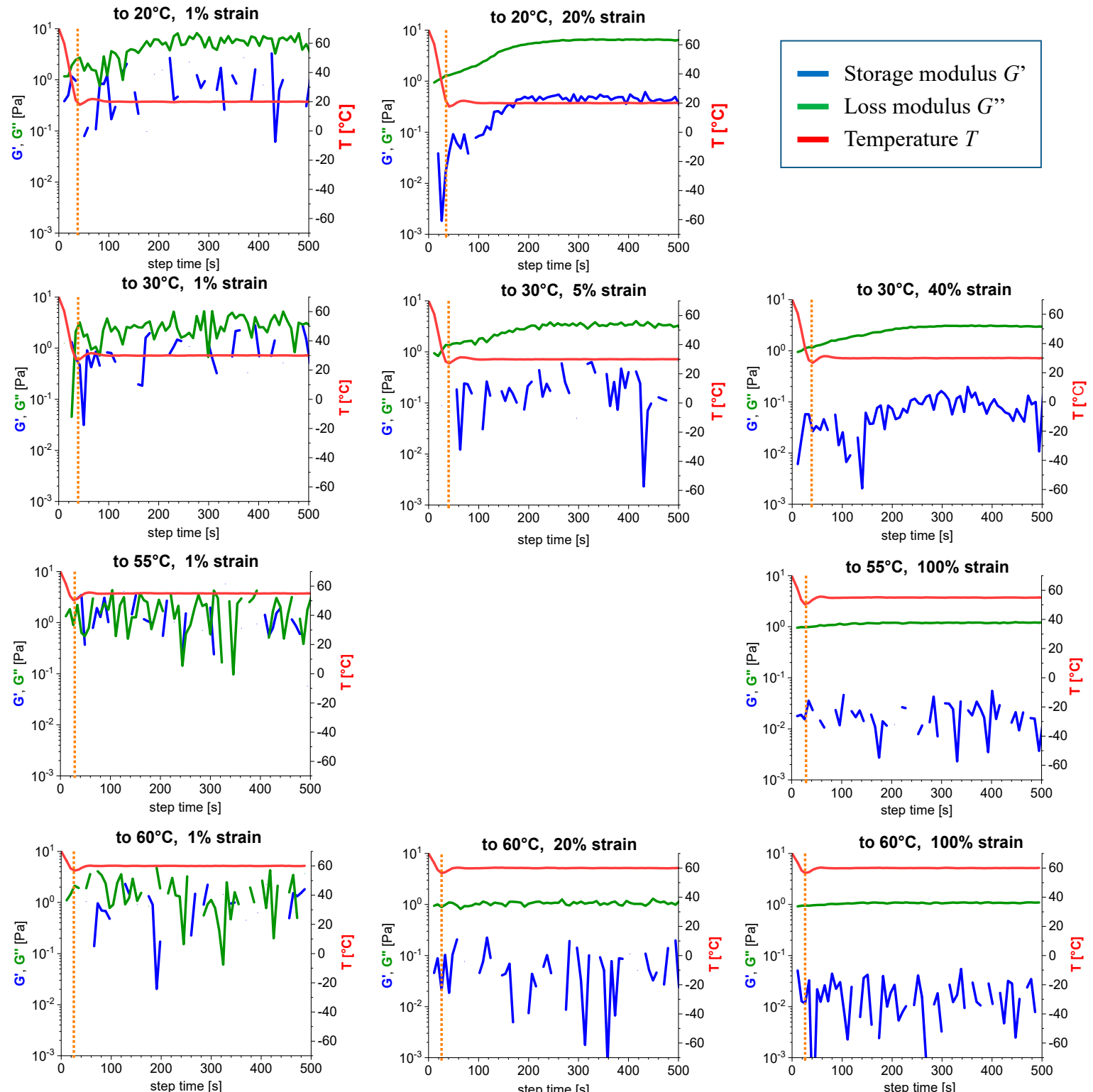
SI-Fig. 18: Thixotropy effects as strain-dependence – study of very low strains – of the moduli values and curve course – especially G' , less so G'' , in case of the kinetics of physical gelation of molten H03–BAFKU₂ upon abrupt cooling.

H11-BAFKU₂ kinetics of gelation upon cooling



SI-Fig. 19: Thixotropy effects visible as strong strain-dependence of the moduli values (G' , G'') in case of the kinetics of physical gelation of molten H11-BAFKU₂ upon abrupt cooling.

H21-BAFKU₂ kinetics of gelation upon cooling

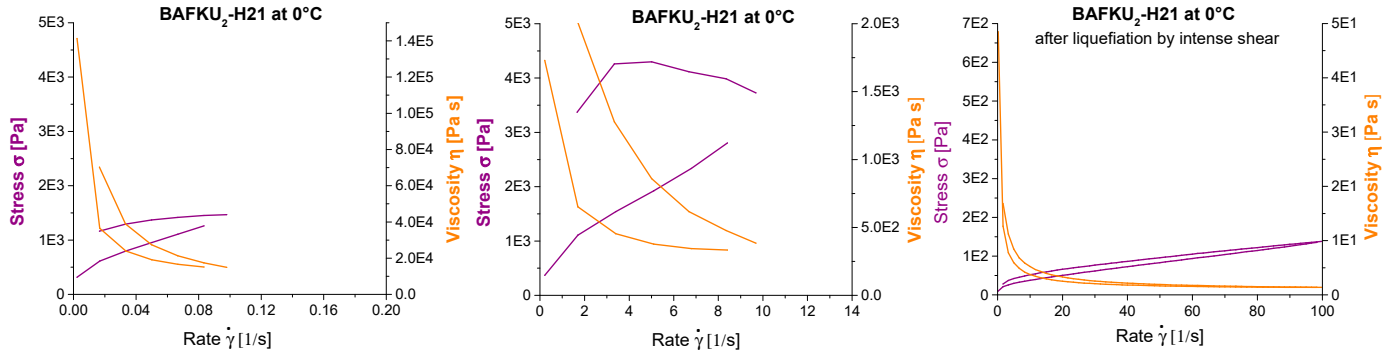


SI-Fig. 20: Thixotropy effects visible as strong strain-dependence of the moduli values (G' , G'') in case of the kinetics of physical gelation of molten H21-BAFKU₂ upon abrupt cooling.

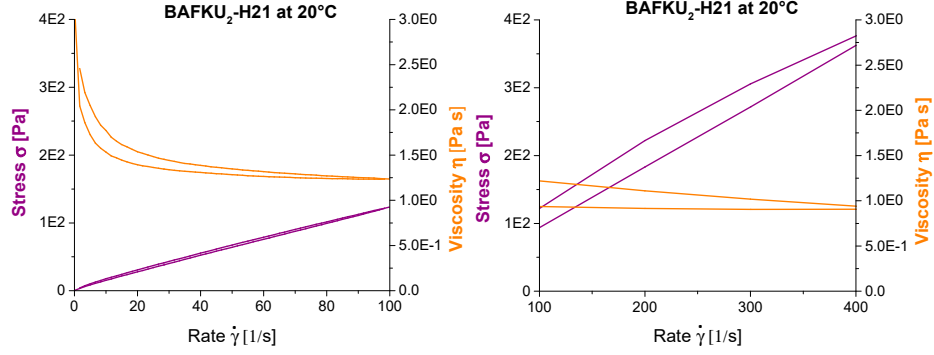
Thixotropic Loop tests

H21-BAFKU2

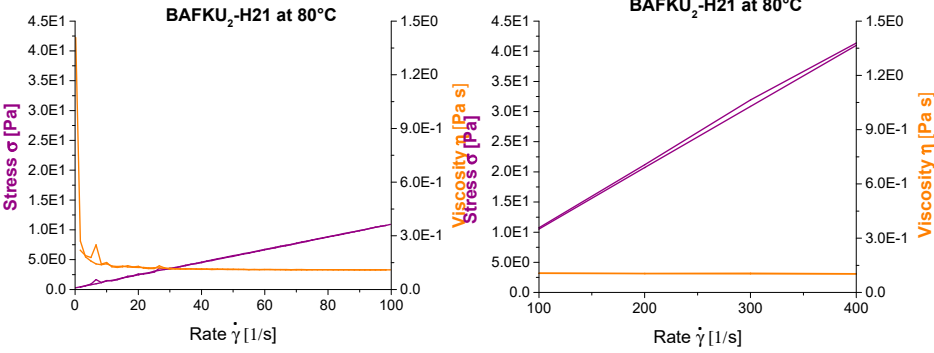
0°C



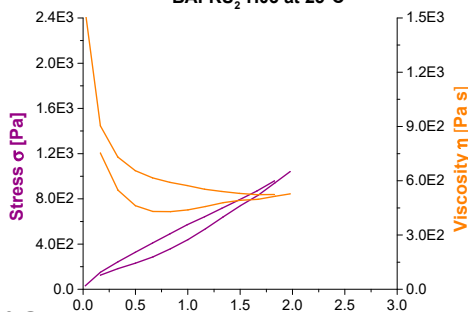
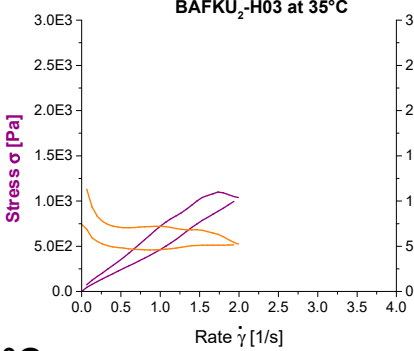
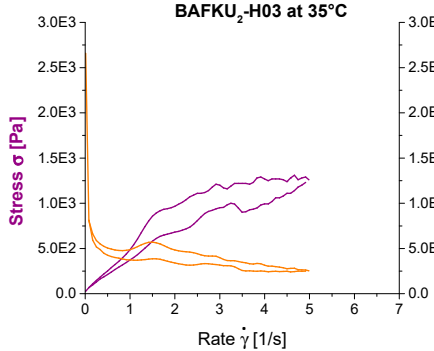
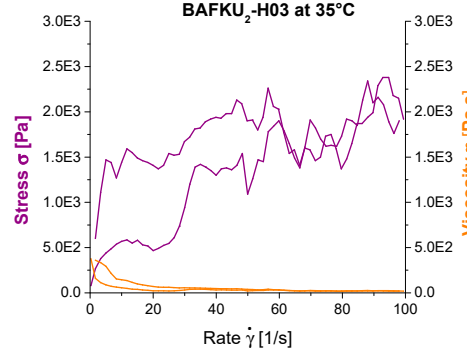
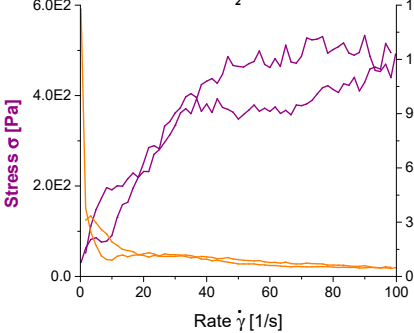
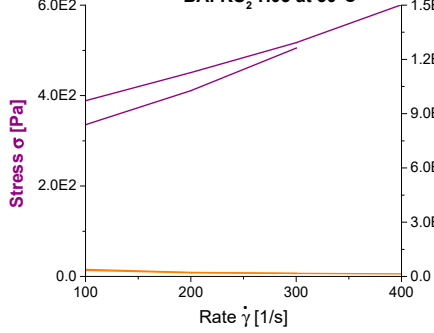
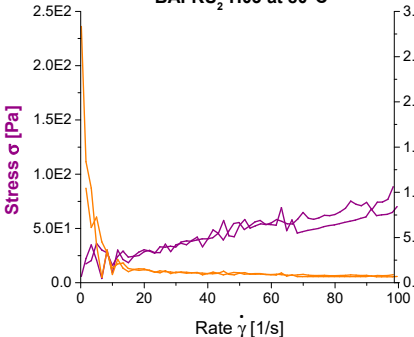
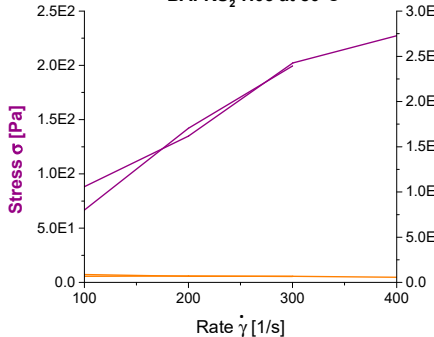
20°C



80°C



SI-Fig. 21: Thixotropic loop tests (dependence of shear stress and of viscosity on the shear rate) for the copolymer H21–BAFKU₂ at 0, 20 and 80°C: at the left are continuous tests with shear rates rising up to 100 s⁻¹, at the right are step-wise tests with shear rates between 100 and 400 s⁻¹.

H03-BAFKU2**25°C****BAFKU₂-H03 at 25°C****35°C****BAFKU₂-H03 at 35°C****BAFKU₂-H03 at 35°C****BAFKU₂-H03 at 35°C****50°C****BAFKU₂-H03 at 50°C****BAFKU₂-H03 at 50°C****80°C****BAFKU₂-H03 at 80°C****BAFKU₂-H03 at 80°C**

SI-Fig. 22: Thixotropic loop tests (dependence of shear stress and of viscosity on the shear rate) for the copolymer H03–BAFKU₂ at 25, 35, 50 and 80°C: at the left are continuous tests with shear rates rising up to 100 s⁻¹, at the right are step-wise tests with shear rates between 100 and 400 s⁻¹; at 35°C, only 100 s⁻¹ could be reached, but two low-shear-rates tests were performed.